Oxidation States, Transport Properties, and Te···Te Short Contacts in the Ternary Transition Metal Tellurides $Ta_3Pd_3Te_{14}$ and $Ta_4Pd_3Te_{16}$

Pere Alemany,*,† Stéphane Jobic,‡ Raymond Brec,‡ and Enric Canadell*,§

Departament de Química-Física, Universitat de Barcelona, Diagonal 647, 08028 Barcelona, Spain, Institut des Matériaux de Nantes, 2 rue de la Houssinière, BP 32229, 44322 Nantes Cedex 03, France, and Institut de Ciència de Materials de Barcelona (CSIC), Campus de la UAB, 08193 Bellaterra, Spain

Received May 9, 1997[⊗]

The electronic structures of the layered ternary tellurides $Ta_3Pd_3Te_{14}$ and $Ta_4Pd_3Te_{16}$ are examined. It is found that the presence of bicapped trigonal prismatic chains with extensive Te···Te interactions results in very wide tellurium-based bands along the direction of the chains. The local octahedral coordination of the Pd and one type of Ta atoms, as well as additional short Te···Te contacts, allows for the participation of the remaining chains of the layer in such a delocalization. This leads to large tellurium to metal electron transfers and difficulties in proposing meaningful oxidation states for the Pd and Ta atoms. The interlayer Te···Te interactions are found to exert a strong control of the density of states at the Fermi level and, hence, of the conductivity of these phases. The results are also compared with those for Ta_3SiTe_6, a structurally different layered ternary telluride with short Te···Te contacts. For this phase, meaningful oxidation states for the Ta and Si atoms can be proposed. The different, but important, role of interlayer Te···Te interactions in Ta_3SiTe_6 is also discussed.

1. Introduction

The chemistry of transition metal tellurides has experienced a remarkable development during the last decade.[1−9] Tellurides are quite different from sulfides and selenides in both structure and properties, and this is what makes tellurium chemistry so appealing. One of the reasons for the uniqueness of transition metal tellurides lies in the very diffuse nature of the tellurium orbitals, which allows the interaction between tellurium atoms, which can be quite far apart. As recently shown,[3b,10] this often leads to tellurium to metal electron transfers which can play an important role in determining the structure and properties of these solids. For instance, the layered system $NbTe_2$, in which Nb is formally d^1 according to the chemical formula, exhibits a structure with double zigzag chains which would be the expected one if Nb was formally $d^{4/3}$.[11] Indeed calculations show that there are many Te···Te interlayer contacts shorter than the sum of the van der Waals radii which lead to the overlap of the Te p-block bands and the Nb d-block bands, i.e., to the required Te → Nb electron transfer.[11]

According to recent band structure calculations, the Te···Te nonbonding contacts responsible for the overlap of the Te p-block bands and the metal d-block bands can be as long as 3.75 Å.[3b,d,e,10,12] This is the reason why such interactions were usually disregarded in the past. These calculations have also shown that the distance alone is not a good indicator of the effectiveness of a Te···Te interaction: the directionality of the interacting Te orbitals is also very important. The depopulation of the top of the Te p-block bands, which is the region where

† Universitat de Barcelona.
‡ Institut des Matériaux de Nantes.
§ Institut de Ciència de Materials de Barcelona (CSIC).
⊗ Abstract published in *Advance ACS Abstracts,* October 1, 1997.

(1) (a) Liimatta, E. W.; Ibers, J. A. *J. Solid State Chem.* **1987**, *71*, 384. (b) Liimatta, E. W.; Ibers, J. A. *J. Solid State Chem.* **1988**, *77*, 141. (c) Liimatta, E. W.; Ibers, J. A. *J. Solid State Chem.* **1989**, *78*, 7. (d) Mar, A.; Ibers, J. A. *J. Chem. Soc., Dalton Trans.* **1991**, 639. (e) Keane, P. M.; Lu, Y.-J.; Ibers, J. A. *Acc. Chem. Res.* **1991**, *24*, 223. (f) Mar, A.; Ibers, J. A. *J. Am. Chem. Soc.* **1993**, *115*, 3227. (g) Mar, A.; Ibers, J. A. *J. Solid State Chem.* **1991**, *92*, 352. (h) Mar, A.; Ibers, J. A. *J. Solid State Chem.* **1992**, *97*, 366. (i) Keane, P. M.; Ibers, J. A. *Inorg. Chem.* **1991**, *30*, 1327. (j) Keane, P. M.; Ibers, J. A. *Inorg. Chem.* **1991**, *30*, 3096. (k) Keane, P. M.; Ibers, J. A. *J. Solid State Chem.* **1991**, *93*, 291. (l) Mitchell, J. F.; Burdett, J. K.; Keane, P. M.; Ibers, J. A.; DeGroot, D. C.; Hogan, T.; Schindler, J. L.; Kannewurf, C. R. *J. Solid State Chem* **1992**, *99*, 103. (m) Cody, J. A.; Ibers, J. A. *Inorg. Chem.* **1994**, *33*, 2713. (n) Mansuetto, M. F.; Cody, J. A.; Chien, S.; Ibers, J. A. *Chem. Mater.* **1995** *7*, 894. (o) Pell, M. A.; Ibers, J. A. *J. Am. Chem. Soc.* **1995**, *117*, 6284.

(2) (a) Badding, M. E.; DiSalvo, F. J. *Inorg. Chem.* **1990**, *29*, 3952. (b) Li, J.; Hoffmann, R.; Badding, M. E.; DiSalvo, F. J. *Inorg. Chem.* **1990**, *29*, 3943. (c) Li, J.; Badding, M. E.; DiSalvo, F. J. *Inorg. Chem.* **1992**, *31*, 1050. (d) Li, J.; Badding, M. E.; DiSalvo, F. J. *J. Less-Common Met.* **1992**, *184*, 257.

(3) (a) Jobic, S.; Brec, R.; Rouxel, J. *J. Solid State Chem.* **1992**, *96*, 169. (b) Jobic, S.; Deniard, P.; Brec, R.; Rouxel, J.; Jouanneaux, A.; Fitsch, A. *Z. Anorg. Allg. Chem.* **1991**, *598/599*, 199. (c) Monconduit, L.; Evain, M.; Boucher, F.; Brec, R.; Rouxel, J. *Z. Anorg. Allg. Chem.* **1992**, *616*, 177. (d) Canadell, E.; Monconduit, L.; Evain, M.; Brec, R.; Rouxel, J.; Whangbo, M.-H. *Inorg. Chem.* **1993**, *32*, 10. (e) Evain, M.; Monconduit, L.; van der Lee, A.; Brec, R.; Rouxel, J.; Canadell, E. *New J. Chem.* **1994**, *18*, 215. (f) van der Lee, A.; Evain, M.; Monconduit, L.; Brec, R.; Petricek, V. *Inorg. Chem.* **1994**, *33*, 3032. (g) Evain, M.; Monconduit, L.; Brec, R. *J. Solid State Chem.* **1995**, *119*, 394.

(4) (a) Park, Y.; Kanatzidis, M. G. *Chem. Mater.* **1991**, *3*, 781. (b) Park, Y.; Degroot, D. C.; Schindler, J.; Kannewurf, C. R.; Kanatzidis, M. G. *Angew. Chem., Int. Ed. Engl.* **1991**, *30*, 1325. (c) Zhang, X.; Li, J.; Foran, B.; Lee, S.; Guo, H.-Y.; Hogan, T.; Kannewurf, C. R.; Kanatzidis, M. G. *J. Am. Chem. Soc.* **1995**, *117*, 10513. (d) Li, J.; Guo, H.-Y.; Zhang, X.; Kanatzidis, M. G. *J. Alloys Comp.* **1995** *218*, 1.

(5) (a) Lee, S.; Nagasundaram, N. *Chem. Mater.* **1989**, *1*, 597. (b) DiMasi, E.; Foran, B.; Aronson, M. C.; Lee, S. *Chem. Mater.* **1994**, *6*, 1867.

(6) (a) Tremmel, W. *Angew. Chem., Int. Ed. Engl.* **1991**, *30*, 840. (b) Tremmel, W. *J. Chem. Soc., Chem. Commun.* **1991**, 1405. (c) Tremmel, W. *Angew. Chem. Int. Ed. Engl.* **1992**, *31*, 217. (d) Tremmel, W. *Inorg. Chem.* **1992**, *31*, 755.

(7) (a) Ahn, K.; Hughbanks, T. R.; Rathnayaka, K. D. D.; Naugle, D. G. *Chem. Mater.* **1994,** *6*, 418. (b) Abdon, R.; Hughbanks, T. R. *Chem. Mater.* **1994**, *6*, 424.

(8) (a) Li, J.; Carroll, P. J. *Mater. Res. Bull.* **1992**, *27*, 1073. (b) Li, J.; Guo, H.-Y.; Proserpio, D. M.; Sironi, A. *J. Solid State Chem.* **1995**, *117*, 247.

(9) (a) Huang, J.; Huang, B. *Jiegou Huaxue* **1988**, *7*, 214. (b) Huang, B.; Huang, J.; Liu, S. *Jiegou Huaxue* **1989**, *8*, 145.

(10) Canadell, E.; Jobic, S.; Brec, R.; Rouxel, J.; Whangbo, M.-H. *J. Solid State Chem.* **1992**, *99*, 189.

(11) Whangbo, M.-H.; Canadell, E. *J. Am. Chem. Soc.* **1992**, *114*, 9587.

(12) Canadell, E.; Mathey, Y.; Whangbo, M.-H. *J. Am. Chem. Soc.* **1988**, *110*, 104.

S0020-1669(97)00554-5 CCC: $14.00

the more antibonding Te···Te levels are found, is characterized by the appearance of weak but positive Te···Te overlap populations. Although apparently weak, these Te···Te interactions lead to important modifications in the band structure which are responsible for the above mentioned tellurium to metal electron transfers.

Such electron transfers complicate the electron counting arguments based on usual oxidation states which are used to rationalize the structure and transport properties of many solids. The situation can be particularly complex in ternary tellurides. Some of these systems are layered compounds with many short intra- and interlayer Te···Te contacts. In addition, there can be relatively short metal to metal contacts which further complicate the situation.[13−14] The more prominent feature of many of these ternary tellurides is the existence of very short intralayer Te···Te contacts which, in view of the previous comments, should have a strong influence on their electronic structures. Ternary transition metal tellurides often display metallic conductivity. Because they are low-dimensional in structure, it is tempting to believe that they could exhibit some of the remarkable physical properties of low-dimensional metals. Thus it is very important to understand how Te···Te and metal···metal interactions influence their electronic structure.[15]

In this work we address the electronic structure of two ternary tellurides: $Ta_3Pd_3Te_{14}$[1c] and $Ta_4Pd_3Te_{16}$.[1d] Their crystal structures are strongly related and contain a large number of very short Te···Te contacts. $Ta_3Pd_3Te_{14}$ contains layers resulting from the condensation of Pd-based octahedral chains, Ta-based trigonal prismatic chains, and Ta-based octahedral chains. $Ta_4Pd_3Te_{16}$ contains layers resulting from the condensation of Pd-based octahedral chains, Ta-based trigonal prismatic chains, and Ta-based *double* octahedral chains. The two phases exhibit metallic conductivity (i.e., the resistivity vs temperature curve has a negative slope) but despite the very close structural relationship, the conductivity of the second phase is one order of magnitude larger.[1c,d] Is there any simple reason to explain this difference? Being low-dimensional metals, why do these phases not exhibit low-temperature resistivity anomalies? Although such questions are quite interesting by themselves, our main concern here will be the relationship between the short Te···Te contacts and the formal oxidation states. We will approach this question by carrying out extended Hückel tight-binding band structure calculations.[16] This type of calculation has been very useful in understanding the electronic structure of several transition metal binary and ternary tellurides.[1f,2b,3d,e,10−14] The exponents and parameters used in the present work are summarized in Table 1. In order to broaden the scope of our discussion, we will also compare the results with those for layered ternary tellurides like Ta_3SiTe_6, whose layers are structurally quite different.[3e]

Table 1. Exponents and Parameters Used in the Calculations[a]

atom	orbital	H_{ii} (eV)	ζ_1	ζ_2	c_1[b]	c_2[b]
Ta[c]	6s	−10.10	2.28			
	6p	−6.86	2.24			
	5d	−12.10	4.76	1.94	0.6597	0.5589
Pd[d]	5s	−9.20	2.19			
	5p	−5.30	2.15			
	4d	−12.90	5.98	2.61	0.5264	0.6372
Te	5s	−20.78	2.51			
	5p	−13.20	2.16			

[a] A modified Wolfsberg−Helmholz formula (Ammeter, J.; Bürgi, H-B.; Thibeault, J.; Hoffmann, R. *J. Am. Chem. Soc.* **1978**, 100, 3686) was used to calculate the off-diagonal H_{ij} values. [b] Contraction coefficients used in the double-ζ expansion. [c] Reference 15a. [d] Reference 17. [e] Reference 12.

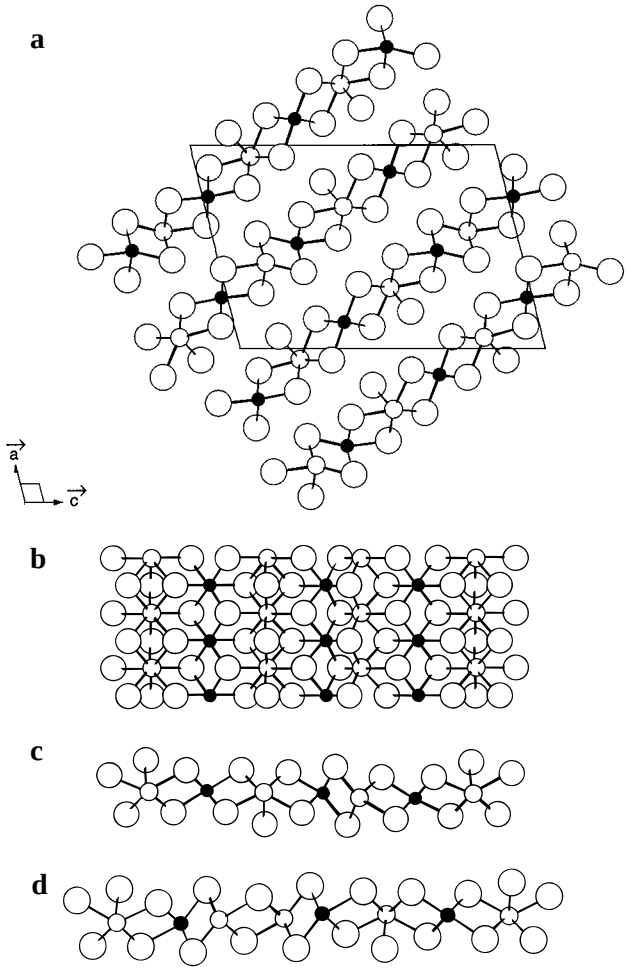

Figure 1. (a) Projection view of the crystal structure of $Ta_3Pd_3Te_{14}$ along the *b* axis. (b) View of a $Ta_3Pd_3Te_{14}$ layer along a direction perpendicular to the slab. (c) Projection view of one layer of $Ta_3Pd_3Te_{14}$ along the *b* axis. (d) Projection view of one layer of $Ta_4Pd_3Te_{16}$ along the *b* axis. In all drawings small empty circles represent Ta atoms, small filled circles represent Pd atoms, and large empty circles represent Te atoms.

2. Crystal Structure

Shown in Figure 1a is a projection along the *b* axis of the crystal structure of $Ta_3Pd_3Te_{14}$. Although not shown in the figure, there are several Te···Te short contacts between the $Ta_3Pd_3Te_{14}$ layers (3.514, 3.651, 3.666, 3.685, etc). Several of these contacts are noticeably shorter than those leading to the above mentioned tellurium to metal electron transfers (∼3.75 Å). A view of one $Ta_3Pd_3Te_{14}$ layer along a direction perpendicular to the slab is shown in Figure 1b. In order to discuss the electronic structure of this phase it is essential to clearly understand first its crystal structure. As can be seen from Figure 1a,b, there are successively six different chains of three different types along the slab. The first type is a Ta-based trigonal prismatic chain (Ta-TP). These chains are made of $TaTe_6$ trigonal prisms sharing their two opposite triangular faces. A top view of this $TaTe_3$ chain is shown in **1**. The second structural motif in the layer consists of Pd-based octahedral chains (Pd-OCT). These chains are built from $PdTe_6$ octahedra

(13) Halet, J.-F.; Hoffmann, R.; Tremmel, W.; Liimatta, E. W.; Ibers, J. A. *Chem. Mater*. **1989**, *1*, 451.
(14) Mar, A.; Jobic, S.; Ibers, J. A. *J. Am. Chem. Soc.* **1992**, *114*, 8963.
(15) The same situation can occur in some ternary selenides. See, for instance: (a) Canadell, E.; Whangbo, M.-H. *Inorg. Chem*. **1987**, *26*, 3974. (b) Alemany, P.; Jobic, S.; Brec, R.; Canadell, E. Manuscript in preparation.
(16) Whangbo, M.-H.; Hoffmann, R. *J. Am. Chem. Soc*. **1978**, *100*, 6093.
(17) Doublet, M.-L.; Canadell, E.; Whangbo, M.-H. *J. Am. Chem. Soc*. **1994**, *116*, 2115.

by sharing two opposite edges. **2** is a top view of these $PdTe_4$ chains. The final structural motif in the layers is a Ta-based

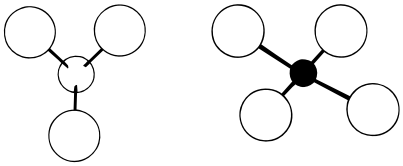

1 **2**

$TaTe_4$ edge-sharing octahedral chain (Ta-OCT) **3**. As can be seen in Figure 1a,b, the assembling of the layer from these three types of chains is done in such a way that every Ta-based chain has two adjacent Pd-based chains and vice versa. In addition, the Ta atoms in trigonal prismatic coordination form two additional bonds with Te atoms of the adjacent Pd-OCT chains. Thus, these Ta atoms are really in a bicapped trigonal prismatic environment so that in the following we will refer to them as Ta-BTP chains (**4**). Within these layers there are a large number of very short intralayer Te···Te contacts (3.125, 3.147, 3.209, 3.268, 3.355 Å, etc).

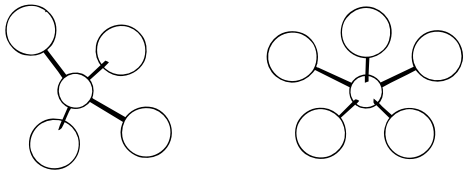

3 **4**

The $Ta_4Pd_3Te_{16}$ phase is also a layered system, and the layers are strongly related to those of $Ta_3Pd_3Te_{14}$. As shown in Figures 1c,d where we present top projection views of the $Ta_3Pd_3Te_{14}$ and $Ta_4Pd_3Te_{16}$ layers, respectively, the main difference is that the *single* Ta-OCT chains in $Ta_3Pd_3Te_{14}$ are replaced by *double* Ta-OCT chains in $Ta_4Pd_3Te_{16}$. Thus, these two phases can be considered to be the simplest members of a hypothetical large family of phases. $Ta_4Pd_3Te_{16}$ also exhibits short interlayer (3.637, 3.774 Å, etc.) and intralayer (3.060, 3.221, 3.373 Å, etc.) Te···Te contacts. It is worth mentioning that the triangular faces of the $TaTe_6$ prisms (see Figure 1c) are not equilateral but isosceles with one very short Te···Te distance (3.061 Å). This distance is not far from that of a full $(Te-Te)^{2-}$ single bond (∼2.90 Å).[18] In $Ta_3Pd_3Te_{14}$ there are two slightly different trigonal prismatic chains where these Te···Te distances, although a little bit longer, are still very short (3.125 and 3.147 Å). It should be mentioned that in both phases there are relatively short Pd···Ta distances (3.110 Å in $Ta_3Pd_3Te_{14}$ and 3.073 Å in $Ta_4Pd_3Te_{16}$) between adjacent octahedral chains. These distances are suggestive of some metal−metal bonding.

3. Electronic Structure

Assuming the usual oxidation states of Ta^{5+} for Ta-OCT, Ta^{5+} for Ta-BTP, and Pd^{4+} for Pd-OCT, the charge cannot be balanced for $Ta_3Pd_3Te_{14}$ if tellurium is assumed to be Te^{2-}. This is in agreement with the metallic behavior of $Ta_3Pd_3Te_{14}$ and suggests that the origin of such behavior is the existence of holes in the Te p-block bands. However, using the same oxidation states the charge can be perfectly balanced for $Ta_4Pd_3Te_{16}$, so that the question arises as to why this system is also metallic. One possibility is that the top occupied and bottom empty bands really slightly overlap, leading to a semimetallic behavior. This could be favored by the short Te···Te contacts. However, the close structural relationship between the two systems suggests that things are probably not so simple. If the average oxidation state of tellurium in $Ta_3Pd_3Te_{14}$ is smaller than Te^{2-}, why should this not also be the case in $Ta_4Pd_3Te_{16}$? A careful analysis of the band structure of these systems is needed before any understanding of the origin of their transport properties can be attempted.

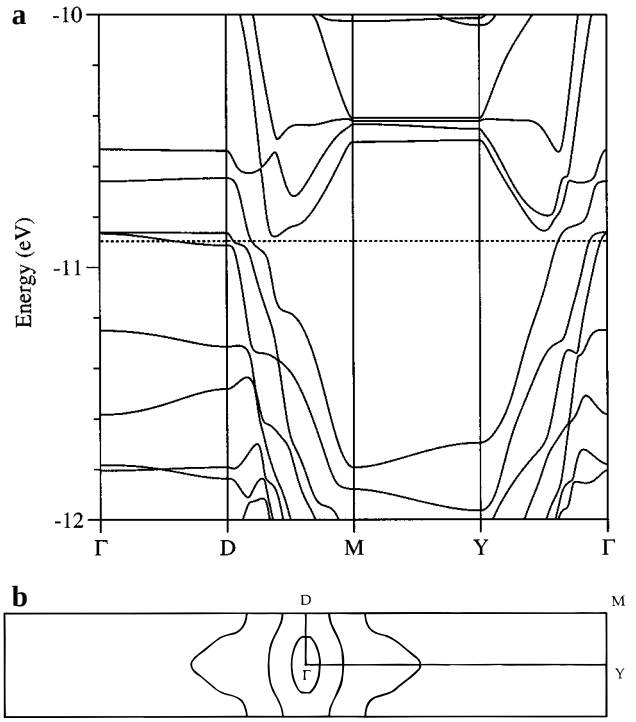

Figure 2. (a) Band structure calculated for an isolated $Ta_3Pd_3Te_{14}$ layer where the dashed line refers to the Fermi level. The Γ, D, Y, and M labels refer to the wave vector points (0, 0), ($d^*/2$, 0), (0, $b^*/2$), and ($d^*/2$, $b^*/2$), respectively, and d is defined as $d = a + c$. (b) Calculated Fermi surfaces for an isolated $Ta_3Pd_3Te_{14}$ layer.

A. Band Structure of $Ta_3Pd_3Te_{14}$. The calculated band structure for an isolated $Ta_3Pd_3Te_{14}$ slab is shown in Figure 2a. Here it should be noted that whereas the b axis corresponds to one of the main directions of the slab (i.e., direction of the chains), the interchain direction perpendicular to b is $a + c$ (=d). Thus the Γ → Y direction in Figure 2a can be associated with the interactions along the chains whereas the Γ → D direction can be associated with the interchain interactions within the slab. As shown in Figure 2a the Fermi level cuts very dispersive bands so that the system is predicted to be metallic. The important result of Figure 2a is that there are a large number of very dispersive bands along the direction of the chains. These bands cross other less dispersive bands along the same direction, and because of the resulting avoided crossings, the band structure along Γ → Y (as well as along D → M) looks quite complicated. These very dispersive bands are heavily based on the tellurium orbitals. It is clear that we are quite far from a situation in which the top of the tellurium p-block bands and the bottom of the appropriate metal d-block bands can be clearly distinguished (either slightly overlapping or being separated by a band gap). This situation is associated with a strong electron reorganization and important tellurium to metal electron transfers. Before looking carefully at the implications of this result, let us point out two other interesting aspects of the band structure of Figure 2a. First, the interchain interactions are much weaker than those along the chains. However, although difficult to recognize from Figure 2a because of the many avoided crossings, they are non-negligible for two of the three bands crossing the Fermi level (this can be traced back to the dispersion of the two lowest bands shown along M → Y). This leads to the quite warped (or even closed for the third band) Fermi surfaces shown in

(18) Bronsema, K. D.; van Smaalen, S.; de Boer, J. L.; Wiegers, G. A.; Jellinek, J.; Mahy, J. *Acta Crystallogr., Sect. B* **1987**, *43*, 305.

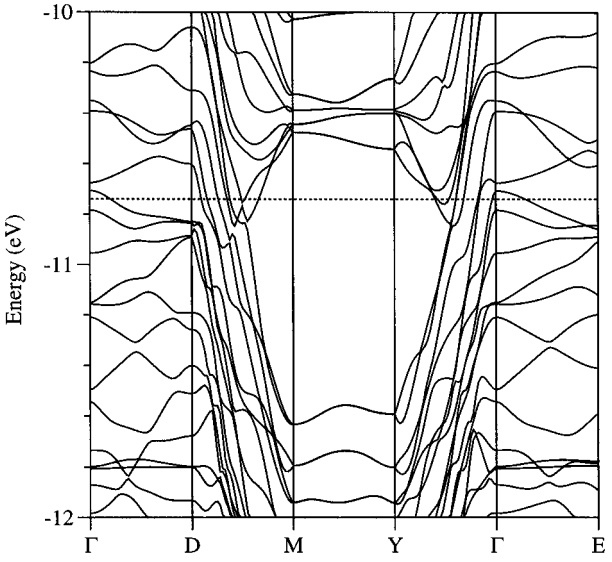

Figure 3. Calculated band structure for the three-dimensional structure of $Ta_3Pd_3Te_{14}$ where the dashed line refers to the Fermi level. The Γ, D, Y, M, and E labels refer to the wave vector points (0, 0, 0), ($d^*/2$, 0, 0), (0, $b^*/2$, 0), ($d^*/2$, $b^*/2$, 0) and (0, 0, $e^*/2$), respectively, and d is defined as $d = a + c$. The e vector is defined so as to be perpendicular to the layers.

Figure 2b, which preclude the possibility of a Fermi surface driven electronic instability and the corresponding resistivity anomaly.[19,20] We will come back to this problem later on. The second observation is that there are empty bands exhibiting a minimum very close to the Fermi level (see the Γ → Y and D → M directions of Figure 2a). Thus, small shifts of the Fermi level can have an important effect on the density of states at the Fermi level. This can have a noticeable influence on the conductivity of the system. Since the bands around the Fermi level have a strong tellurium content, it is clear that the interlayer Te···Te contacts could lead to such Fermi level shifts and, consequently, be very important in governing the conductivity of this phase.

Selected lines for the calculated three-dimensional (3D) band structure of $Ta_3Pd_3Te_{14}$ are shown in Figure 3. The Γ → D and Γ → Y lines have the same meaning as in Figure 2. The Γ → E direction is associated with the interslab interactions along a direction perpendicular to the layers. Because there is more than one slab per unit cell, Figure 3 looks very complex as a result of the many bands in the diagram. However, a comparison shows that, except for the multiplication of bands, Figures 2 and 3 are not that different. There are, however, three important modifications brought about by the switching of the interlayer interactions which can be readily seen in Figure 3. First, the band dispersion along the interchain direction of the slab (see Γ → D in Figures 2a and 3) has clearly increased. Second, the band dispersion along the direction perpendicular to the slabs (see Γ → E in Figure 3) is also important. Third, although hidden through many avoided crossings, the empty bands exhibiting a minimum along the Γ → Y and D → M directions in Figure 2a are crossed by the Fermi level and thus are partially filled. This leads to a complex 3D Fermi surface containing more contributions than that of the single layer. More importantly, the dispersion acquired by the bands crossing the Fermi level along both the interchain and interslab directions leads to important warpings for the different pieces of the Fermi surface. The result is a very complex Fermi surface with several closed and very warped pieces which make unlikely any Fermi surface driven instability like charge density wave, for instance.[19,20] Thus it is understandable that $Ta_3Pd_3Te_{14}$ is a normal metal without any apparent anomaly in the resistivity vs temperature curve.

It is clear from our discussion that the intralayer Te···Te interactions play an extremely important role in determining the band structure near the Fermi level. These intralayer interactions are responsible for the existence of the very wide tellurium-based bands which, as it will be discussed later, are the more characteristic features of the band structure of $Ta_3Pd_3Te_{14}$ (and $Ta_4Pd_3Te_{16}$). However, it is also important to emphasize the significant role of the Te···Te interlayer interactions. They not only reinforce the warping of the Fermi surface and thus lead to a very stable metallic state but also have an important role in shifting some of the bands crossed by or near the Fermi level. Accordingly they significantly affect the density of states at the Fermi level, which has an effect in determining the conductivity of the system. From a chemical viewpoint, these band shifts are associated with electron transfers between the tellurium and transition metal atoms. How both the intralayer and interlayer Te···Te contacts regulate such electron transfers is something we must carefully analyze before concluding anything about the formal oxidation states of Ta, Pd, and Te.

B. Oxidation States and Te···Te Short Contacts in $Ta_3Pd_3Te_{14}$. The band structures of Figures 2a and 3 are too complex to be examined in detail. In order to consider what are the more likely oxidation states of the Ta-OCT, Ta-BTP, and Pd atoms it is more convenient to look at the density of states of 3D $Ta_3Pd_3Te_{14}$, as well as the partial contributions of these atoms. The total and partial densities of states are reported in Figure 4a−c. Also shown in each panel of Figure 4 is the integrated partial density of states.

Let us comment first on the Pd contribution to the density of states (Figure 4a). Since Pd is in an octahedral environment, we should expect that the partial density of states of Pd exhibits a peak associated with the three t_{2g} levels of every Pd, a smaller contribution (higher in energy) associated with the e_g^* levels, and finally, another contribution (lower in energy) associated with the e_g levels. In fact, the Pd contribution to the density of states (see Figure 4a) can be seen as the superposition of a sharp peak (around −13 eV) and a very broad contribution between −8 and −16 eV. The peak is associated with the t_{2g} levels while the broad contribution arises from the e_g and e_g^* levels, which are very delocalized. Such delocalization complicates the determination of an appropriate oxidation state for the Pd atoms. The integrated density of states up to the Fermi level corresponds to a practically neutral Pd atom. However, this cannot be taken as an indication that Pd is found as d^{10} because the integrated density of states contains all the Pd contributions to the bonding levels. The oxidation state gives a rough description of the occupation of the e_g and e_g^* levels. In view of Figure 4a, we believe that the more reasonable way to tackle this problem is to divide the wide contribution in two parts: that below the t_{2g} peak can be attributed to the e_g levels, and that above the t_{2g} peak to the e_g^* ones. Under such assumptions, the Pd atoms would have the e_g^* levels approximately half-filled and the oxidation state could be Pd^{2+}. In other words, there is a noticeable electron transfer from tellurium to palladium.

Before discussing how appropriate the above proposal is, let us consider the Ta contributions. The partial density of states for Ta-OCT is shown in Figure 4b. Since there is just one Ta-OCT per every three Pd atoms, the partial density of states of

(19) Wilson, J. A.; DiSalvo, F. J.; Mahajan, S. *Adv. Phys.* **1975**, *24*, 117.
(20) Canadell, E.; Whangbo, M.-H. *Chem. Rev.* **1991**, *91*, 965.
(21) The existence of some stacking faults in the real structure of Ta_3SiTe_6[3e] was disregarded in our calculations. Thus, the unit cell of 3D Ta_3SiTe_6 contains two symmetry-related Ta_3SiTe_6 layers.

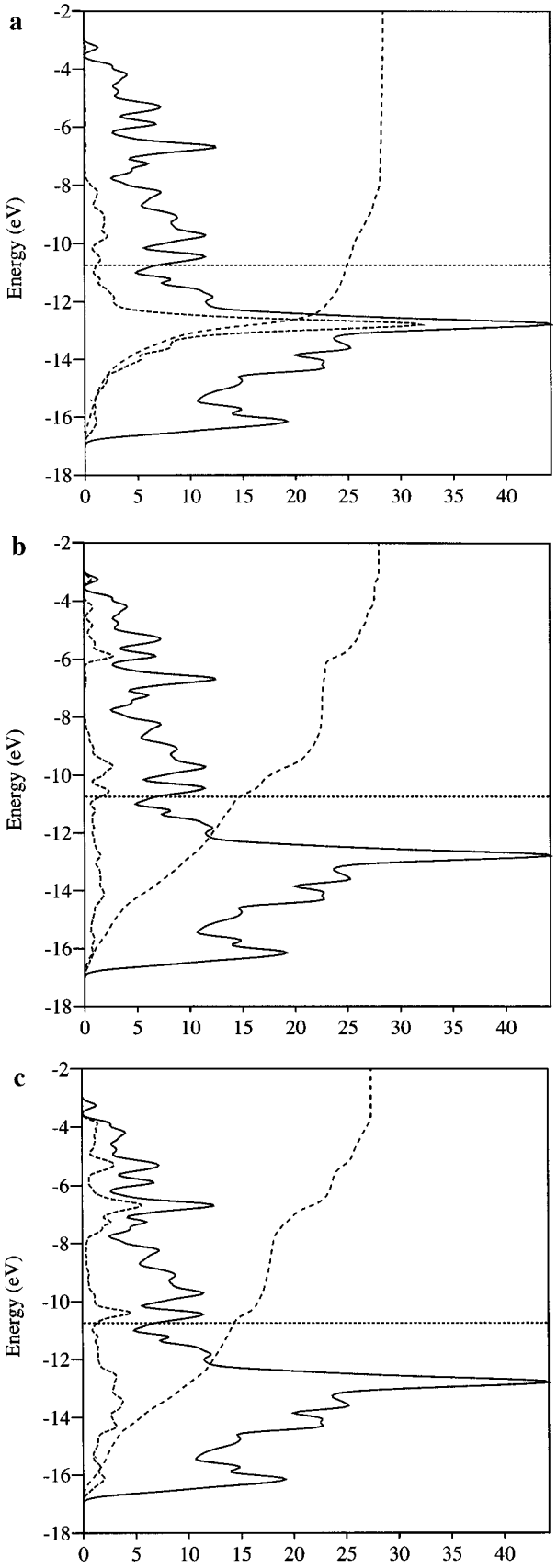

Figure 4. Total (continuous line) and partial (broken line) density of states plots for the three-dimensional structure of $Ta_3Pd_3Te_{14}$. The partial densities of states in panels a, b, and c are those of Pd-OCT, Ta-OCT, and Ta-BTP, respectively. Also shown in the plots are the integrated partial densities of states. The horizontal dashed lines refer to the Fermi level.

Figure 4b is smaller in absolute value than that of Figure 4a. Even if both the Pd and Ta-OCT atoms have the same octahedral environment, the corresponding contributions to the density of states are quite different. For Ta-OCT we can recognize the contribution of the e_g* levels between −4 and −6 eV, which is well separated from another wide contribution from −8 to −16 eV. It is not easy to distinguish the t_{2g} and e_g levels from this wide region, and consequently, we believe that any proposition of an oxidation state for Ta-OCT would be quite arbitrary. In any event, it is clear that we are not in a situation which could justify the use of the Ta^{5+} oxidation state.

The partial density of states for Ta-BTP is reported in Figure 4c. As discussed by Hoffmann and co-workers one should expect a one-below-four levels pattern for this coordination geometry.[13] Again, it is not possible to recognize the expected pattern from the partial density of states of Figure 4c. Even recognizing the problems in relating electron densities and oxidation states, it is difficult to reconcile a Ta^{5+} oxidation state with the fact that half of the d levels of Ta-BTP are filled, according to the integrated density of states. It is clear that there is a non-negligible electron transfer from tellurium to Ta-BTP. As for Ta-OCT, we believe that because of the strong delocalization it is not possible to propose safely a definite oxidation state for the tantalum atoms. In fact, only the Pd t_{2g} levels seem to be immune to the very large delocalization. We believe that the notion of oxidation state is not quite meaningful in this phase.

What is the cause of the problem? One cause is the presence of the very dispersive tellurium bands noted in the previous section. The origin of these bands is to be found in the bicapped triangular prismatic chains of the layers. The zigzag chains formed by the capping and triangular Te atoms lead to a very strong σ-type overlap between the tellurium p orbitals parallel to the chain (**5**) and lead to the above mentioned very dispersive bands. However, although this is the main cause, it is not the

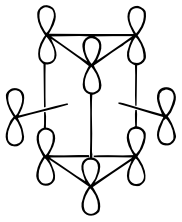

5

only one. After all, the dispersive tellurium bands could undergo weakly avoided crossings with the mainly metal based levels, and in that case the problem would disappear. The Ta-BTP and Pd-OCT chains are strongly coupled for two reasons. First, the capping and two of the triangular tellurium atoms of the Ta-BTP chains belong also to the octahedral environment of the Pd atoms. Thus, the very wide Te bands incorporate Pd character (especially e_g and e_g*). Second, as described in section 2, one of the Te−Te triangular sides of the Ta-BTP chains, i.e., that parallel to the layer, is quite short. The calculated overlap population (∼0.18) is, however, noticeably smaller than that typical for a full Te−Te bond (∼0.50). Although short (3.125 and 3.147 Å in the two slightly different Ta-BTP chains), the distance is long enough for the Te−Te σ* to be considerably populated.[13] This leads to the reduced overlap population and, more importantly, introduces considerable Te−Te σ* character below the Fermi level. This couples pairs of Pd-OCT chains and the Ta-BTP and Pd-OCT chains. In a certain way, the $Ta_3Pd_3Te_{14}$ layers can be considered to be formed by blocks of quintuple chains $Ta_2Pd_3Te_{14}$ coupled through the Ta atoms in the octahedral holes (Ta-OCT). But since all tellurium atoms forming the octahedral environment of these Ta-OCT are part of such $Ta_3Pd_3Te_{14}$ quintuple chains, the Ta-OCT d-block orbitals are also introduced into the very dispersive bands.

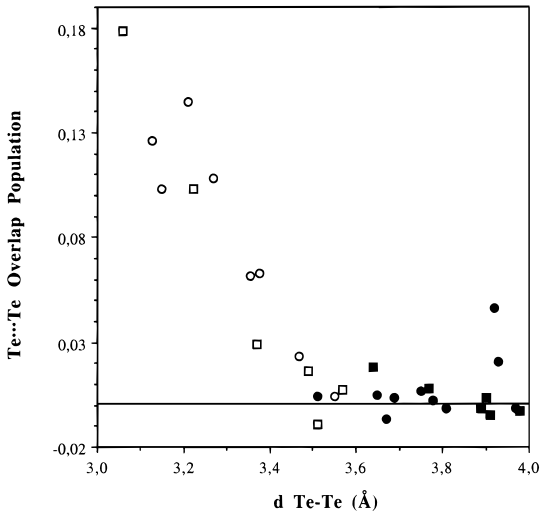

Figure 5. Calculated Te···Te overlap populations vs distance (Å). Empty and filled circles correspond to intra- and interlayer Te···Te contacts in $Ta_3Pd_3Te_{14}$, respectively. Empty and filled squares correspond to intra- and interlayer Te···Te contacts in $Ta_4Pd_3Te_{16}$, respectively.

Parenthetically, it should be noted that there is also some direct interaction between the Pd and Ta atoms of condensed octahedral chains, as shown by a definitely positive overlap population (0.08).

The previous description suggests that the wide bands in the region between −8 and −16 eV must be very delocalized among the Pd-OCT, Ta-BTP, and Ta-OCT chains. This leads to the memory loss of the level splittings associated with the different coordination environments of the transition metal atoms exhibited, at least partially, in Figure 4. In other words, most bonding and antibonding metal−tellurium energy levels resulting from the local environment of the Ta and Pd atoms are partially mixed under the influence of the zigzag tellurium chains in the bicapped trigonal prismatic chains. It seems to us that under such circumstances it is not possible to propose any meaningful oxidation states for the Pd, Ta-OCT, Ta-BTP, and the different Te atoms.

Since the top of the very wide tellurium bands lies higher than the Fermi level, the more antibonding $Ta_3Pd_3Te_{14}$ levels are depopulated and, thus, there must be several positive Te···Te overlap populations. That this is so is clear from the overlap populations reported in Figure 5. Six intralayer Te···Te contacts are associated with quite positive overlap populations. The first two (3.125 and 3.147 Å) are the above mentioned short triangular sides of the Ta-BTP chains. The next four (3.209, 3.268, 3.355, 3.375 Å) are all associated with the zizzag chains of the Ta-BTP chains. These overlap populations are very large compared with those mentioned in the Introduction and thus implicate a very important tellurium to transition metal transfer. All of this is expected from our discussion. The more surprising results of Figure 5 are the quite positive overlap population for two interlayer contacts as large as 3.9−3.95 Å. Many shorter interlayer Te···Te contacts are associated with almost negligible overlap populations. This result clearly illustrates the importance of the interlayer Te···Te contacts discussed in the previous section. It also makes clear that it is not possible to evaluate the importance of these interlayer contacts without carrying out detailed band structure calculations.

C. $Ta_3Pd_3Te_{14}$ vs $Ta_4Pd_3Te_{16}$. Let us now compare the electronic structures of $Ta_3Pd_3Te_{14}$ and $Ta_4Pd_3Te_{16}$. The calculated band structure for an isolated $Ta_4Pd_3Te_{16}$ layer is shown in Figure 6. In order to facilitate the comparison between Figures 2a and 6 we have used the same labeling in both figures, i.e., *b* is the repeat vector along the direction of the chains and

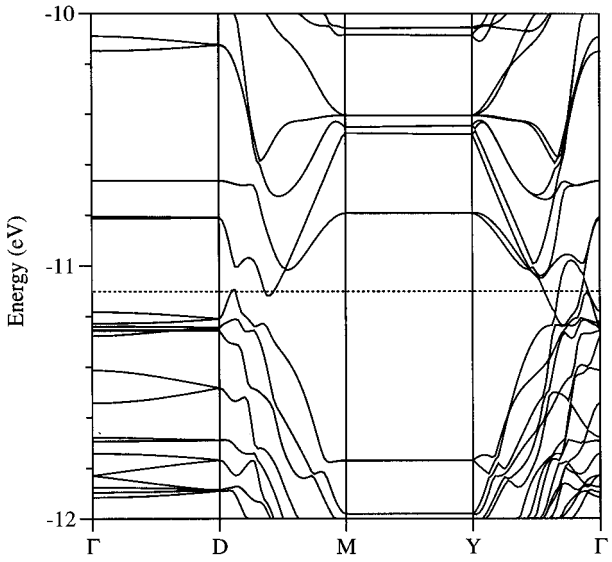

Figure 6. Calculated band structure for an isolated $Ta_4Pd_3Te_{16}$ layer where the dashed line refers to the Fermi level. The Γ, D, Y, and M labels refer to the wave vector points (0, 0), (*d**/2, 0), (0, *b**/2), and (*d**/2, *b**/2), respectively. As in Figure 2, *b* is the repeat vector along the direction of the chains and *d* is a vector perpendicular to *b*.

d is a repeat vector perpendicular to *b*. The unit cell used for the $Ta_4Pd_3Te_{16}$ layer calculations contains two formula units. This is why there seem to be many more bands along the Γ → Y and Γ → D directions of Figure 6 than along the same directions of Figure 2a. Along X → M and M → Y all bands are doubly degenerate. These are artificial consequences of the double cell used in our calculations.

The two figures exhibit a common feature: the very strongly dispersive bands along the direction of the chains (Γ → Y and X → M). Thus, we must expect the same problems we had for $Ta_3Pd_3Te_{14}$ in proposing oxidation states. The main difference between the band structures of the $Ta_3Pd_3Te_{14}$ and $Ta_4Pd_3Te_{16}$ layers is that in the latter the bands displaying a minimum along the direction of the chains cross the Fermi level and are thus partially filled. As discussed in section 3.A, the position of the Fermi level with respect to these bands is very sensitive to the nature and strength of the Te···Te interactions. A comparison of Figures 2a and 6 makes it very clear that, despite the strong structural relationship, the density of states at the Fermi level and consequently, the conductivity of this class of ternary tellurides can be noticeably different and are determined by small differences in the intra- and interlayer Te···Te interactions. As described for $Ta_3Pd_3Te_{14}$, introduction of the interlayer interactions in the calculations further complicates the description of the electronic structure around the Fermi level, leading to very complex and warped Fermi surfaces. Most of the conclusions reached in the two previous sections apply also to $Ta_4Pd_3Te_{16}$ and will not be repeated here.

In the context of the present work the comparison between the $Ta_3Pd_3Te_{14}$ and $Ta_4Pd_3Te_{16}$ phases is more conveniently done by focusing on the total and partial densities of states at the Fermi level reported in Table 2. For $Ta_3Pd_3Te_{14}$ the introduction of the interlayer interactions has only a moderate effect on the density of states at the Fermi level: it decreases by 10%. In contrast, the effect in $Ta_4Pd_3Te_{16}$ is very large: an increase of 46%. Two points must be emphasized here. First, the density of states at the Fermi level is considerably higher for $Ta_4Pd_3Te_{16}$. This is in very good agreement with the fact that the conductivity of $Ta_4Pd_3Te_{16}$ is one order of magnitude larger than that of $Ta_3Pd_3Te_{14}$. Such an increase in the density of states at the Fermi level is mostly associated with the Te contribution and secondarily with the Pd one. The Pd contribu-

Table 2. Fermi Level (ϵ_f) as Well as Total ($N(\epsilon_f)$) and Partial ($N_{Pd}(\epsilon_f)$, $N_{Ta-BTP}(\epsilon_f)$, $N_{Ta-OCT}(\epsilon_f)$, and $N_{Te}(\epsilon_f)$) Densities of States[a] at the Fermi Level for Isolated Layers and the 3D Structures of $Ta_3Pd_3Te_{14}$ and $Ta_4Pd_3Te_{16}$

	$Ta_3Pd_3Te_{14}$		$Ta_4Pd_3Te_{16}$	
	layer	3D	layer	3D
ϵ_f (eV)	−10.896	−10.743	−11.102	−10.868
$N(\epsilon_f)$	3.776	3.383	3.739	5.466
$N_{Ta-BTP}(\epsilon_f)$	0.759	0.651	0.493	0.676
$N_{Ta-OCT}(\epsilon_f)$	0.844	0.758	1.294	1.321
$N_{Pd}(\epsilon_f)$	0.524	0.551	0.601	1.066
$N_{Te}(\epsilon_f)$	1.649	1.422	1.352	2.403

[a] The densities of states are given in electrons per eV and per formula unit.

tion practically did not contribute to the moderate decrease in the case of $Ta_3Pd_3Te_{14}$. Second, although the changes in the density of states at the Fermi level are considerably more important for $Ta_4Pd_3Te_{16}$, examination of Figure 5 suggests that the interlayer interactions should be more important for $Ta_3Pd_3Te_{14}$. There is no contradiction between the two results. In the first case we are examining the influence of the interlayer interactions just around the Fermi level. This is important to understand differences in conductivity among the two phases. In the second case we are examining the effect of the interlayer interactions in all occupied levels. This is important to understand the nature of the Te to metal electron transfers. Our calculations highlight the very important role of the Te···Te interlayer interactions in understanding the conductivity of layered ternary tellurides where very dispersive tellurium bands cross the Fermi level. We suspect that they are also very important in order to understand the striking differences in conductivity of the $MM'Te_5$ (M = Ni, Ta; M′ = Pd, Pt) phases.[1g]

D. $Ta_3Pd_3Te_{14}$ and Ta_3SiTe_6: Comparison of the Electronic Structures of Two Structurally Very Different Layered Ternary Tellurides. Our analysis of the electronic structure of $Ta_3Pd_3Te_{14}$ and $Ta_4Pd_3Te_{16}$ suggests that it is difficult to propose definite oxidation states to the different transition metal atoms. In fact, similar problems were found by Hoffmann and co-workers[13] in their study of the electronic structure of another type of ternary transition metal tellurides, $NbMTe_5$ (M = Ni, Pd). Thus, one could be tempted to think that this is a quite general result for ternary transition metal tellurides. However, this is not so. That the usual oxidation state formalism is valid or not for ternary transition metal tellurides depends on the actual crystal structure of the system. In this section we would like to illustrate this point by considering the electronic structure of Ta_3SiTe_6, a layered ternary telluride for which it is possible to propose definite oxidation states to the atoms.

Shown in Figure 7 is a top projection view of one of the layers in Ta_3SiTe_6. The metal atoms are in a trigonal prismatic coordination. There are three kinds of Ta atoms in each Ta_3SiTe_6 layer: those of the Ta_2Te_8 double prismatic units (Ta_2 and Ta_3) and those of the $TaTe_6$ single prisms (Ta_1). The Ta_2Te_8 double prismatic units are fused to form chains along the *a* direction, and the chains are interconnected by the $TaTe_6$ single prisms. The $TaTe_6$ single prisms and Ta_2Te_8 double prisms are capped by Si atoms. This telluride possesses numerous intra- and interlayer short Te···Te contacts. In fact Ta_3SiTe_6 is one member of a large family of layered compounds (MA_xTe_2 (M = Nb, Ta; A = Si, Ge; $^1/_3 \leq x \leq {}^1/_2$) built from the same structural blocks.[3g]

The calculated band structure for an isolated Ta_3SiTe_6 layer is shown in Figure 8a whereas that for the 3D system is shown in Figure 8b. A detailed analysis of density of states for 3D Ta_3SiTe_6 shows that in both cases the Si 3s contributions occur well below the Fermi level while the Si 3p contributions occur well above. Thus, the oxidation state appropriate for Si is Si^{2+}. Our calculations also show that the atomic populations for the three different Ta atoms are almost identical, suggesting that their oxidation states are also the same. The contribution of the Ta orbitals to the levels around the Fermi level is quite important. Calculations for $TaTe_6$ single prisms and Ta_2Te_8 double prisms and comparison with the band structure calculations clearly show that one d-block level of the $TaTe_6$ single prisms and two d-block levels of the Ta_2Te_8 double prisms are lying low enough to be filled.[22] Thus the oxidation states of the three Ta atoms can appropriately be described as Ta^{3+}. Using the oxidation states Ta^{3+} and Si^{2+}, the average oxidation state for the tellurium atoms should be $Te^{1.833-}$. Thus, in order to

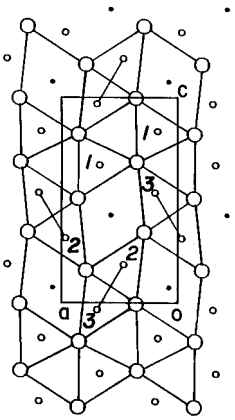

Figure 7. Projection view along the *b* axis of one layer in the crystal structure of Ta_3SiTe_6. The large and small empty circles represent Te and Ta atoms whereas the filled circles represent Si atoms. The three different types of Ta atoms are also indicated.

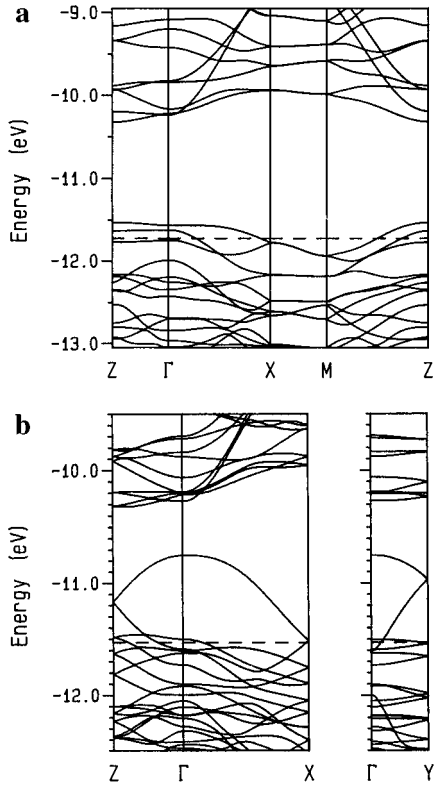

Figure 8. Calculated band structure for (a) a single layer of Ta_3SiTe_6 (Γ = (0, 0), X = (a^*/2, 0), Z = (0, c^*/2), and M = (a^*/2, c^*/2)) and (b) the three-dimensional structure of Ta_3SiTe_6 (Γ = (0, 0, 0), X = (a^*/2, 0, 0), and Z = (0, 0, c^*/2)). The dashed lines refer to the Fermi level.

(22) For a more detailed analysis of this point, see refs 3d and 3e.

be sure that the oxidation states suggested by our study are correct we should also verify that every six Te^{2-} lose one electron in our calculations.

Let us now come back to the band structure of Figure 8a (i.e., the band structure of an isolated Ta_3SiTe_6 layer). As can be seen in Figure 7, the repeat unit of the layer contains two formula units. With an electron counting of $(Ta_3SiTe_6^-)_2$ per unit cell, all of the band levels below the band gap in Figure 8a would be filled. Since there is one electron less per formula unit, the higher bands are partially filled. If these bands were mostly tellurium in character, the origin of the $Te^{1.833-}$ average oxidation state for tellurium would be clear. However, this is not so because the partially filled levels of the layer have also a strong Ta 5d character. Consequently, the introduction of the interslab Te···Te contacts must play a very important role in adjusting the electron counting of Ta_3SiTe_6 by raising one band per layer with strong Te character above the Fermi level. In fact, comparing panels a and b of Figure 8 it is easy to see that this is really what happens. Let us recall that the unit cell of 3D Ta_3SiTe_6 contains two layers.[22] A comparison of the two band structures of Figure 8 shows that two bands (i.e., one band per layer) are very strongly raised in energy so that they largely occupy the forbidden energy region of the single layer. As expected, these bands are mainly tellurium in character. Since we are just discussing the formal oxidation states of the atoms, the fact that there is not a band gap in some parts of the Brillouin zone is not important for our argument. Interestingly, this semimetallic type overlap should confer metallic properties to Ta_3SiTe_6. The essential point of our discussion is that formal oxidation states can be proposed and understood in the case of Ta_3SiTe_6.

What is the difference between $Ta_3Pd_3Te_{14}$ and Ta_3SiTe_6? In both compounds there are many Te···Te short contacts within and between the layers. As discussed in section 3.A, the problems in proposing oxidation states to the transition metal atoms arise from the presence of the extremely wide Te-based bands along the direction of the chains. These bands are so wide that they cross (and consequently mix with) many transition metal based bands leading to the quite complicated situation described in sections 3.A and 3.B. This is not the case in Ta_3SiTe_6, in which case the small readjustment needed to balance the charges is brought about by the interlayer Te···Te interactions. This does not mean that the intralayer interactions are not important. They prepare the raising up of the two bands needed to adjust the charge by pushing quite high in energy one Te-based band per layer with orbital character well oriented toward the adjacent layer. Then, interlayer Te···Te interactions come into play and lead to the final, balanced electron distribution with the nonintegral average oxidation state on Te but well-defined integral oxidation states for the transition metal atoms. As discussed in section 3.B, the origin of the extremely wide Te-based bands of $Ta_3Pd_3Te_{14}$ and $Ta_4Pd_3Te_{16}$ is to be found in the zigzag tellurium chains formed by the capping and triangular Te atoms of the Ta-BTP chains. The type of condensation of the prismatic units in the layers of Ta_3SiTe_6 cannot lead to such very dispersive Te-based bands. Thus, the inner structure of the layer is a key factor in determining if a simple and understandable oxidation state formalism can be used for such binary and ternary tellurides.

Of course, the presence of such very wide Te-based bands does not mean that we cannot propose simple oxidation states. It will depend very much on the nature, formal electronegativity, and type of coordination of the transition metal atoms. Depending on the position of some of the transition metal bands with respect to the wide Te bands, the electron transfer can be relatively small so that the usual oxidation states will still be valid for a simplified description of the electronic structure. All that is needed to appropriately describe such cases is to introduce a small band overlap between the tellurium and transition metal bands which, of course will be important to correctly describe the semimetallic (or metallic) properties of the system, but which will not strongly alter the formal oxidation states. Examples of such a situation among binary or ternary tellurides are $ZrTe_3$,[12] β-$MoTe_2$,[23] and $TaIrTe_4$.[14] For layered ternary tellurides it can be anticipated that the presence of capped trigonal prismatic chains and late transition metal atoms in the other chains will invariably lead to problems in proposing meaningful oxidation states. $Ta_3Pd_3Te_{14}$, $Ta_4Pd_3Te_{16}$, and $NbNiTe_5$[13] are three examples. It is clear that the electronic structure of ternary (or quaternary) transition metal tellurides is richer and more complex than that of the ternary sulfides and selenides. However the present work and previous theoretical studies[1f,2a,3d,e,4c,13,14] are providing useful guiding trends which, it is hoped, will ultimately lead to a simple qualitative understanding of their electronic structure and transport properties.

Acknowledgment. This work was partially supported (S.J., R.B., and E.C.) by the European Union Human Capital and Mobility Program (CHRX-CT94-0675). Part of this work was carried out during a visit of E.C. to the Departament de Química Inorgànica, Universitat de Barcelona. E.C. would like to thank Pr. S. Alvarez for his hospitality and the Fundación Iberdrola for a visiting professorship (January through March 1996), which made possible the stay. Financial support (P.A.) was provided by DGYCIT through Grant PB95-0848-C02-01 and CIRIT through Grant GRQ 94-1077. The computing resources of the Centre de Supercomputació de Catalunya (CESCA) were generously made available through a grant from Fundació Catalana per la Recerca and the Universitat de Barcelona.

IC970554B

(23) Canadell, E.; Whangbo M.-H. *Inorg. Chem.* **1990**, *29*, 1398.